Acta Geologica Sinica (English Edition), 2021, 95(2): 602–616

Origin of the Gas Hydrate and Free Gas in the Qilian Permafrost, Northwest China: Evidence from Molecular Composition and Carbon Isotopes

TAN Furong[1, 2, 3, 4, *], LI Yang[1, *], DU Fangpeng[2, 3], LIU Shiming[2, 3], CUI Weixiong[5], LIU Zhiwu[6], GENG Qingming[3] and LU Ping[1]

[1] *State Key Laboratory of Continental Dynamics, Department of Geology, Northwest University, Xi'an 710069, China*
[2] *State Key Laboratory of Organic Geochemistry, Guangzhou Institute of Geochemistry, Chinese Academy of Sciences, Guangzhou 510640, China*
[3] *China National Administration of Coal Geology, Beijing 10038, China*
[4] *Shaanxi Mineral Resources and Geological Survey, Xi'an 710068, China*
[5] *Xi'an Research Institute of China Coal Technology & Engineering Group Corp., Xi'an 710077, China*
[6] *College of Earth Science and Resources, Chang'an University, Xi'an 710054, China*

Abstract: The Qilian permafrost of the South Qilian Basin (SQB) has become a research focus since gas hydrates were discovered in 2009. Although many works from different perspectives have been conducted in this area, the origin of gas from gas hydrate is still controversial. Molecular composition and carbon isotope of 190 samples related to gas hydrates collected from 11 boreholes allowed exploration of genetic type, thermal maturity, biodegradation, as well as gas-source correlation of alkane gases from gas hydrates and free gases. Results indicate that alkane gases biodegraded after the formation of natural gas. According to differences in carbon isotopes of methane and their congeners (CH_4, C_2H_6, C_3H_8), the thermal maturity (vitrinite reflectance, V*R*o) of most alkane gases ranges from 0.6% to 1.5%, indicating a mature to high mature stage. The thermal maturity V*R*o of a small part of alkane gas (in boreholes DK5 and DK6) is higher than 1.3%, indicating a high mature stage. Alkane gases were mainly produced by secondary cracking, consisting of crude oil-cracking gases and wet gases cracking to dry gases. Genetic types of alkane gases are primarily oil-type gases generated from shales and mudstones in the upper Yaojie Formation of Jurassic, with less coal-type gases originated from the mudstones in the Triassic Galedesi Formation and the lower Yaojie Formation of Jurassic. Carbon dioxides associated with alkanes from gas hydrates and free gases indicate the thermal decomposition and biodegradation of organic matter. The origins of natural gases from gas hydrates and free gases shed light on the evaluation of petroleum resource potential, deeply buried sediments, and petroleum resource exploration in the SQB.

Key words: uunconventional energy, gas hydrate, carbon isotope, alkane gas origin, thermal maturity, South Qilian Basin

Citation: Tan et al., 2021. Origin of the Gas Hydrate and Free Gas in the Qilian Permafrost, Northwest China: Evidence from Molecular Composition and Carbon Isotopes. Acta Geologica Sinica (English Edition), 95(2): 602–616. DOI: 10.1111/1755-6724.14650

1 Introduction

Gas hydrate, also called 'combustible ice', is a solid substance formed by natural gas and water at low temperature under high-pressure conditions (Collett et al., 2010; Makogon, 2010). It is widely distributed on land and offshore (Kvenvolden, 1993; Makogon, 2010; Liu et al, 2019). Potential reserves of natural gases from gas hydrates are greater than 1.5×10^{16} m^3, which is equivalent to twice the total amount of other fossil energy sources (including coal, oil, natural gas) (Kvenvolden, 1999; Xiao et al., 2020). Therefore, as an unconventional energy source with high-energy density and pollution-free advantages, gas hydrate has been considered one of the most important potential energy sources for the 21st century (Makogon et al., 2007; Collett, 2010). During the past two decades, more and more research has focused on its formation, storage, exploration, and exploitation (Sun et al., 2020; Lu et al., 2020).

The Qilian permafrost, located in northwestern China, is the first permafrost region where gas hydrates were discovered in middle- and low-latitude alpine permafrost regions (Lu et al., 2020). Many works have been carried out regarding the origin of the alkane gas in the Qilian permafrost, and a consensus that the alkane gas is thermogenetic had been reached (Lu et al., 2010, 2013a; Zhu et al., 2010; Cao et al., 2012; Cheng et al., 2016; Huang et al., 2016; Dai et al., 2017; Tan et al., 2017). However, genetic types and origins of gases from gas hydrates and free gas are still controversial and the following proposals have been made: (1) the alkane gas originated from coal-type gas, which is from Jurassic coal-bearing strata (Zhu et al., 2010; Cao et al., 2012); (2) the alkane gas is derived from oil-type gas, which derives

* Corresponding author. E-mail: tanfurong1308@163.com (TAN Furong); liyangxbdx@163.com (LI Yang)

http://www.geojournals.cn/dzxbcn/ch/index.aspx; https://onlinelibrary.wiley.com/journal/17556724

from the mudstone of upper Triassic strata (Lu et al., 2010, 2013a, 2013b; Huang et al., 2016; Zuo et al., 2016); (3) origin of the alkane gas is related to oil-type gas, which is from mud shale of the Lower Jurassic Yaojie Formation (Dai et al., 2017; Tan et al., 2017; Liu et al., 2020); and (4) the gas from gas hydrates is a mixture of coal-type gas and oil-type gas (Cheng et al., 2016; Zhang et al., 2018).

Recently, gas hydrates, coal-bed gas from the Lower Jurassic and shale gas from the Upper Triassic were discovered in boreholes in the Muli sag of the Southern Qilian Basin (SQB) (Lu et al., 2020). Most boreholes show hydrocarbon generation potential and produce gas. However, the gas generation capabilities vary markedly in different regions, indicating that current understanding of the Upper Triassic and Lower Jurassic source rocks needs to be reassessed. It is acknowledged that genetic types, secondary alteration, thermal maturity of alkane gas and hydrocarbon generation capacity of source rock are crucial in the study of gas origin. Consequently, the following issues, which has not been studied in detail, need to be addressed: (1) the thermal maturity of alkane gases; (2) whether the alkane gases in gas hydrate and the free gas are biodegradable; and (3) whether the alkane gas in gas hydrate and the free gas is from primary cracking gas.

In this contribution, we investigate the geochemical characteristics of gases from gas hydrates and free gases in the Qilian permafrost. Then, the genetic type, biodegradation, thermal maturity of alkane gases from gas hydrate and free gas are investigated to correlate with organic abundance, genetic type, thermal maturity of organic matter from the source rocks in the study area. Our aim is to understand the gas hydrate petroleum system in the Muli sag of the SQB.

2 Geological Setting

The Qilian permafrost layers, with an average thickness of up to 80 m, are widespread in the SQB, Qinghai province, which is located on the Middle–South Qilian Block (Fig. 1). The SQB is adjacent to the Northern Qilian tectonic belt in the north, separated from the Qaidam Basin in the south by the Zongwulong tectonic belt, connected with the Western Qinling tectonic belt in the southeast and connected with the Altyn tectonic belt. The SQB has undergone multi-stage tectonic evolution, including a pre-Carboniferous paleo-continental craton evolutionary stage, a new-continental craton evolutionary stage in the Carboniferous–Triassic, and a residual basin evolutionary stage in the Jurassic–Quaternary (Xiao et al., 2009).

In ascending order, the Galedesi Formation (Fm.), Daxigou Fm. and the Yaojie Fm. were deposited in the SQB in the Late Triassic to Early Jurassic (Norian–Toarcian). The Upper Triassic Galedesi Fm. and the Lower Jurassic Yaojie Fm., widely distributed in the Muli sag, are key hydrocarbon exploration targets with a large resource potential of gas hydrates and coal-bed gases. The Galedesi Fm. is characterized by low-angle contact with the overlying Jurassic Daxigou Fm. and integrated with the Atasi Fm. In the study area, the Galedesi Fm. is subdivided into two parts: (1) an upper part made up of gray-to-black carbonaceous shales, siltstones, silty mudstones is intercalated with fine-grained feldspar sandstones and coal lines or seams; (2) a lower section is composed of light-gray to grayish-white feldspar-quartz sandstones with a small amount of black carbonaceous shales, mudstones, silty mudstones, and coal lines. Similarly, the Yaojie Fm. is subdivided into two: (1) the lower part is mainly composed of grayish-white to dark-gray quartz sandstones, siltstones and dark-gray mudstones, carbonaceous mudstones, and coal seams; (2) the upper part mainly consists of dark-gray fine-grained sandstones, siltstones, mudstones, and oil shales.

Gas hydrate samples were first obtained by drilling from the Qilian permafrost in September 2009. This was another breakthrough after gas hydrates were first collected in the northern South China Sea in May 2007. Since then, many boreholes for gas hydrates have been drilled in the permafrost of the Southern Qilian Basin, as shown in Fig. 1. Drilling results show that gas hydrates were found in boreholes DK-1, DK-2, DK-3, DK-7, DK-8, DK-9, DK-12, and abnormal signs of gas hydrates were found in other boreholes. Generally, gas hydrates and their abnormal signs were mainly located in the Lower Jurassic Yaojie Fm. at depths of 130–500 m, where they are mainly distributed in siltstones, mudstones, and oil shale fracture surfaces with thin layers (Fig. 2) (Wang et al., 2011). Evidence of oil and gas (EOG) was found in some boreholes (Lu et al., 2013c; Cheng et al., 2017), which is consistent with the depth and the stratum of the gas hydrate occurrence layer, suggesting a close relation between EOG and gas hydrates (Lu et al., 2013c).

3 Methods

3.1 Data sources

The components and carbon isotopes of natural gas were collected from the 190 samples from gas hydrate and free gas from boreholes in the Qilian permafrost. These data have been published in various papers from 2009 to 2016. Noteworthy is that these samples were derived from natural gas collected by different methods, such as drainage gas collection, mud degasification, vacuum top air method, hydrate decomposition and drilling test mining. More than 90% experimental samples were tested at the National Geological Experiment Testing Center, Beijing, China.

3.2 Data distribution characteristics

All collected samples are from the Lower Jurassic Yaojie Fm. in the Qilian permafrost region, and their main lithologies are oil shale (53 samples, 28%), mudstone (37, 20%), silty mudstone (25, 13%), muddy powder sandstone (24, 13%), powder sandstone (15, 8%), fine sandstone (17, 9%), medium–coarse-grained deposition (9 medium sandstone, 5%; 5 coarse sandstone, 3%), and two from coal seams. The alkane gas samples primarily come from fine sediments, with a few from medium to coarse sediments (9 medium sandstone, 5%; 5 coarse sandstone, 3%). The data are not a complete test for each sample, which may affect the relative ratio of data in the statistical results. Moreover, the uneven distribution of data might

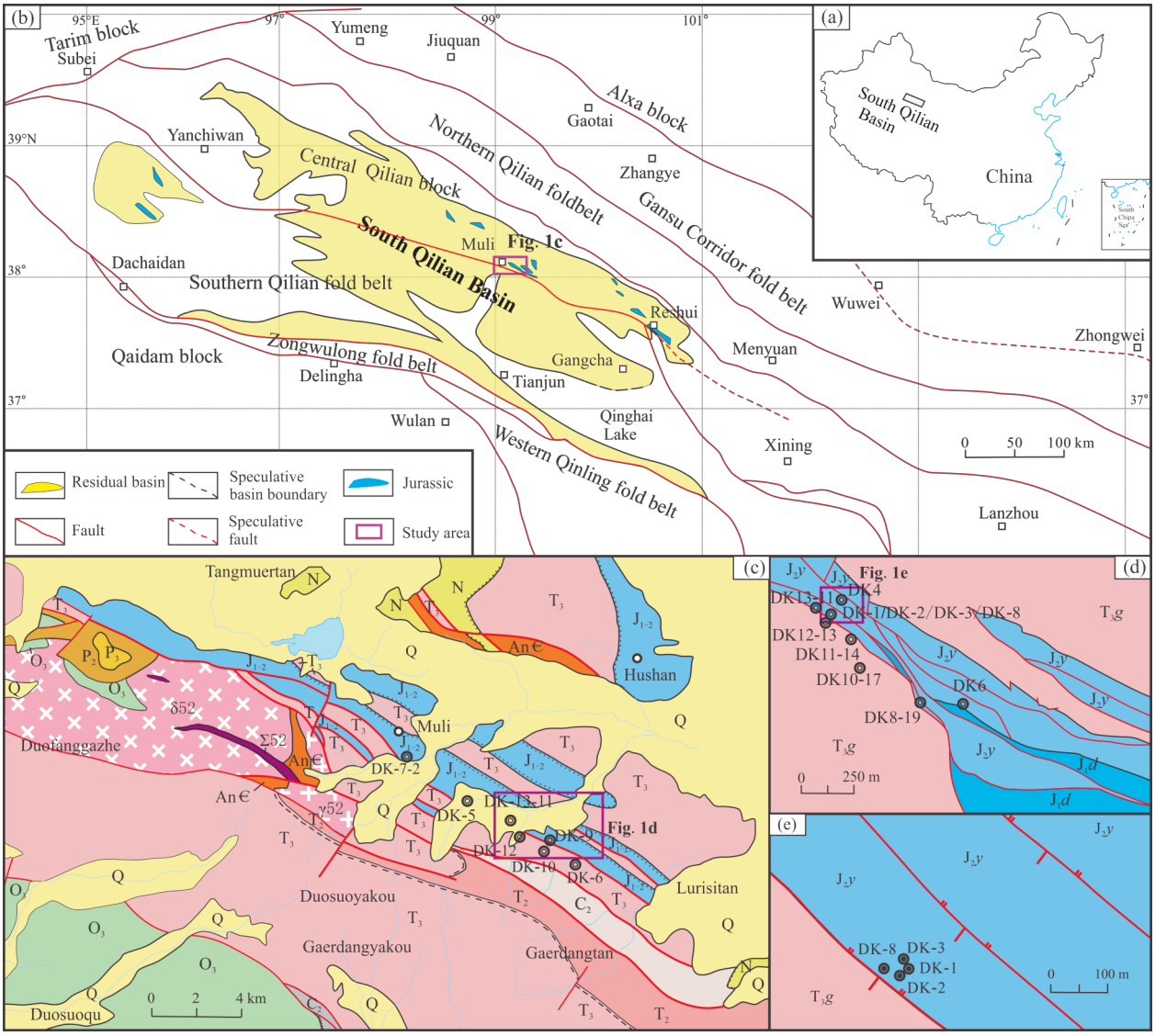

Fig. 1. Diagram of borehole distribution of gas hydrate and free gas in the Qilian permafrost (China base map after China National Bureau of Surveying and Mapping Geographical Information).

lead to amplification or compression of some information. As a result, the data do not fully represent the information and, therefore, it is necessary to discuss the distribution drilling of data.

In this study, we considered molecular composition, carbon isotopes, and hydrogen isotope of the natural gas and so only the distributions of these factors for each hole were analyzed. The distribution of the sample data shows that the molecular components of the alkane gases is mainly from DK8 (85 samples, 45%), DK2 (35, 19%), DK5 (29, 15%) and DK6 (15) (Fig. 3a). Data for the carbon dioxide test of 42 samples were distributed in DK2 (18 samples, 44%), DK12-13 (18, 44%), DK8-19 (6, 15%) (Fig. 3b). Some other carbon dioxide data were distributed in DK1, DK3, DK10-17 and other boreholes, but there were no carbon dioxide samples in DK5 or DK6. The distribution of carbon isotope samples was extremely uneven, 87 samples of methane carbon isotope were from DK8, accounting for more than half of the total data (Fig. 3c). There were fewer ethane carbon isotope samples than methane, with a total of 77 carbon isotope data points, which were from every drill hole in the area (Fig. 3d). A total of 42 propane carbon isotope samples were from DK2, DK12-13, DK8 and DK8-19 (Fig. 3e), but absent in DK5 and DK6.

4 Results

4.1 Chemical composition of gas hydrate and free gas

The histograms of molecular composition of the free gases from the gas hydrate and natural gas in the Qilian permafrost are shown Fig. 4. The molecular components include methane, ethane, propane, butane and pentane. The content of carbon dioxide ranges from 0.05% to 79.40% with an average of 5.62%, and the nitrogen content ranges from 0.23% to 76.76% with an average of 7.62%. The content of the main natural gas component, alkane gas, ranges from 16.50% to 99.90% with an

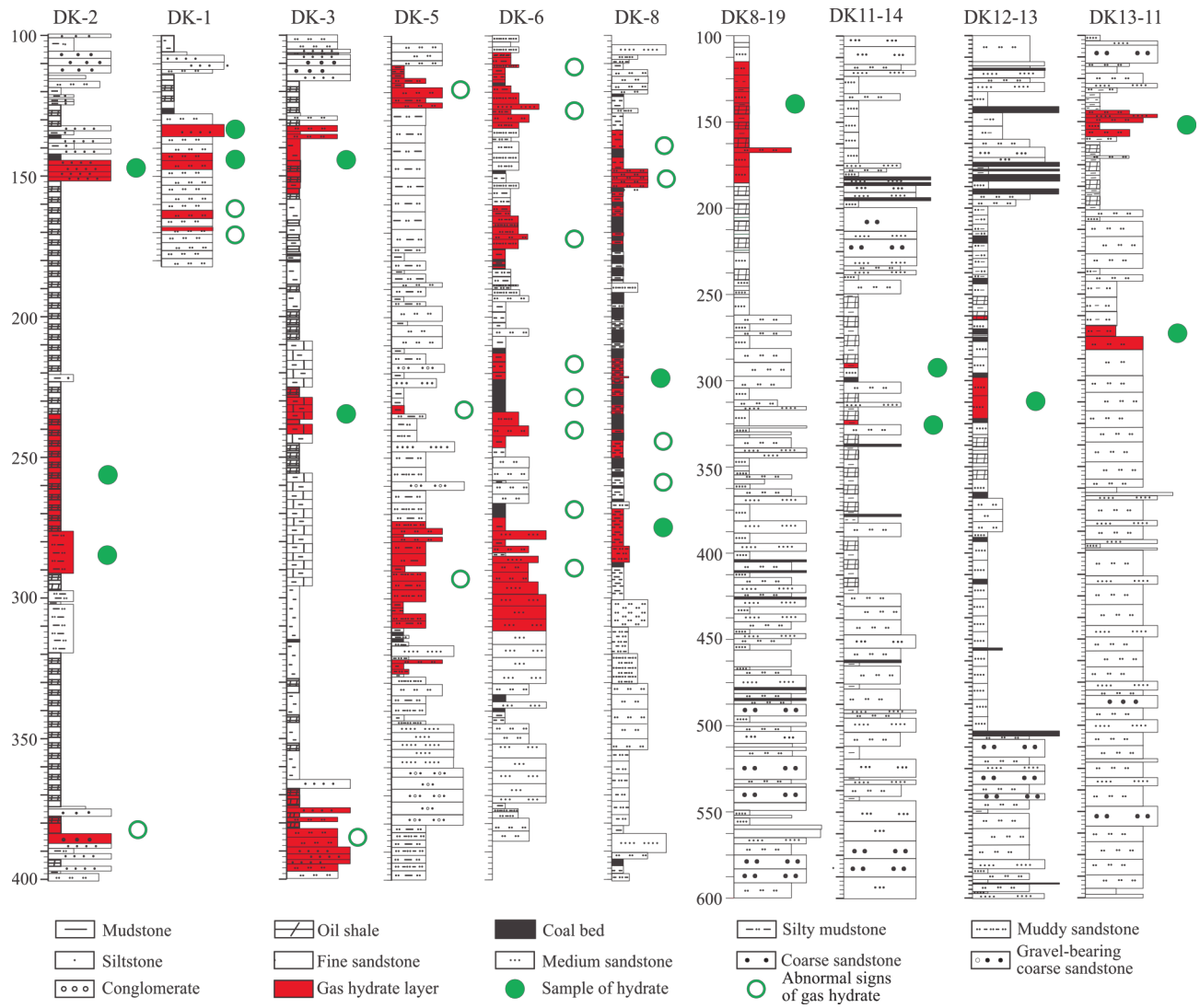

Fig. 2. Distribution profile of gas hydrate and free gas in the Qilian permafrost.

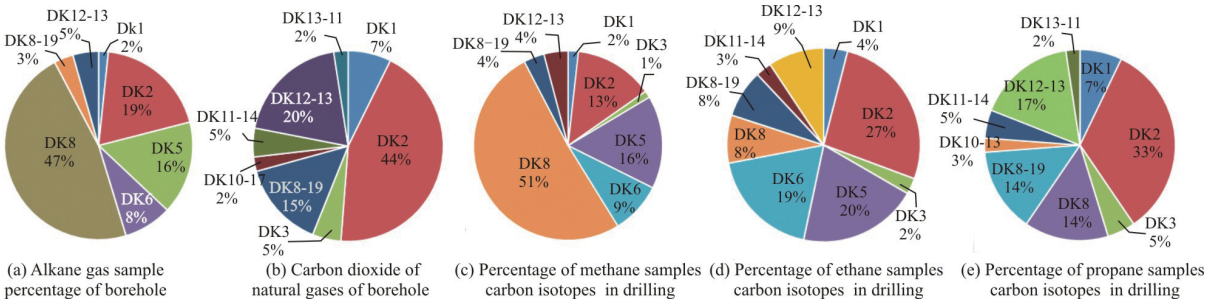

Fig. 3. Molecular composition, borehole distribution and carbon isotope pie chart of alkanes gas from gas hydrate and free gas in the Qilian permafrost.

average of 90.8%.

The molecular composition analysis of 190 natural gas samples obtained from 11 boreholes with different depths shows the dryness coefficients ($C_1/\sum C_{1\text{-}5}$) ranging from 0.18 to 0.99 and mainly concentrated between 0.60 and 0.99, with an average of 0.82. Nearly 40% the dryness coefficients are greater than 0.95 (Fig. 4a). It is noteworthy that the dryness coefficients vary greatly in DK-8 borehole (Fig. 5a). The dryness coefficient of most alkane gas in boreholes DK-5 and DK-6 is higher than 0.95, which implies that the gas is dry. In contrast, most of the dryness coefficient from other boreholes (excepting DK-5, DK-6) do not exceed 0.95, which implies wet gas. Ethane contents of the samples range from 0.16% to 20.57%, mainly between 0.16% and 15%, with an average of 5.44% (Fig. 4b). Propane contents range from 0.01% to

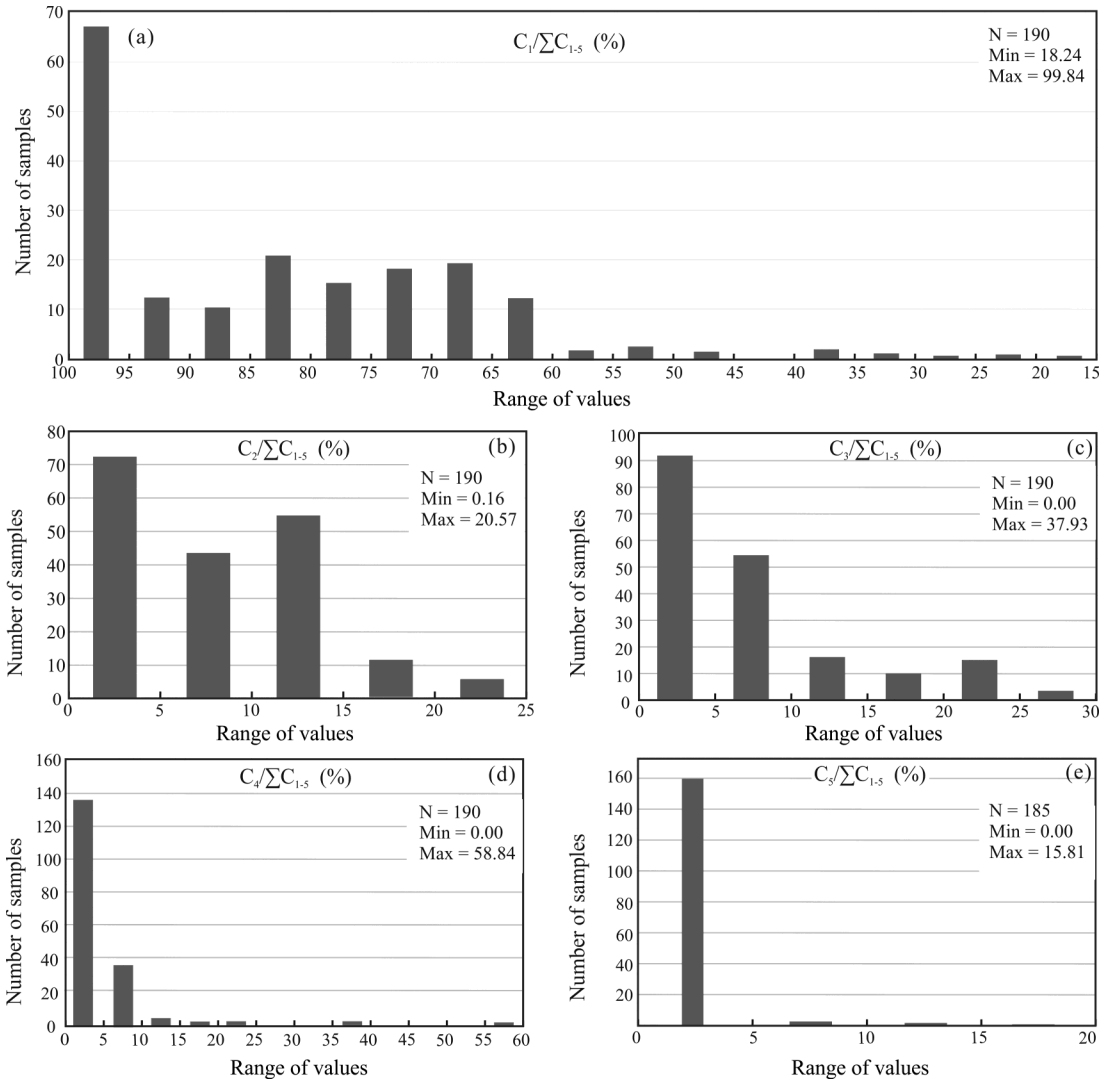

Fig. 4. Frequency distribution of alkanes gas from gas hydrate components in the Qilian permafrost.

37.93%, mainly between 0 and 10%, with an average of 6.7% (Fig. 4c). Butane, including positive butane and isobutane, content ranges from 0.01% to 58.84%, mainly between 0.01% and 10%, with an average of 4.4% (Fig. 4d). Pentane, including n-pentane and isomeric pentane, content ranges from 0.01% to 15.81%, mainly between 0 and 5%, with an average of 0.88% (Fig. 4e).

The factors of secondary microbial transformations, migration, thermal maturity, and genetic type also affect the drying coefficient from the perspective of natural gas accumulation (Quan et al., 2019). The methane-produced anaerobic organisms take priority to consume wet gas, resulting in an increase of the drying coefficient (Milkov, 2011; Milkov and Etiope, 2018). Degradation only takes place in the shallow surface of the earth, and microbial metabolism will stop when the temperature is over 90°C (Milkov, 2011). Therefore, the drying coefficient of alkane gas induced by biodegradation decreases with depth. However, a positive correlation between the drying coefficient of gas and depth is seen for the natural gas from the Qilian permafrost, indicating that biodegradation of microorganisms did not play a dominant role.

Due to the low migration speed of wet gas in low porosity and low permeability rock formations, the drying coefficient of natural gas increases with the migration distance during the migration process (Schoell, 1980). Therefore, if the natural gases from the Qilian permafrost were generated from the Jurassic dark mudstone and coal seams or was gas from Upper Triassic mudstone that migrated to the Middle Jurassic, the drying coefficient should have gradually increased as the depth was reduced. However, the drying coefficient shows a decreasing trend as depth was reduced, indicating that migration fractionation also was not a major factor. Furthermore, as a high-speed migration channel, faults cause formation fractionation to have little effect on natural gas components, making the drying coefficient vary weakly (Ma et al., 1999). However, the natural gas drying coefficient gradually decreases upward in the study area, implying that the natural gas did not migrate vertically through faults. Kerogen genetic type and thermal maturity also play important roles in the drying coefficient of

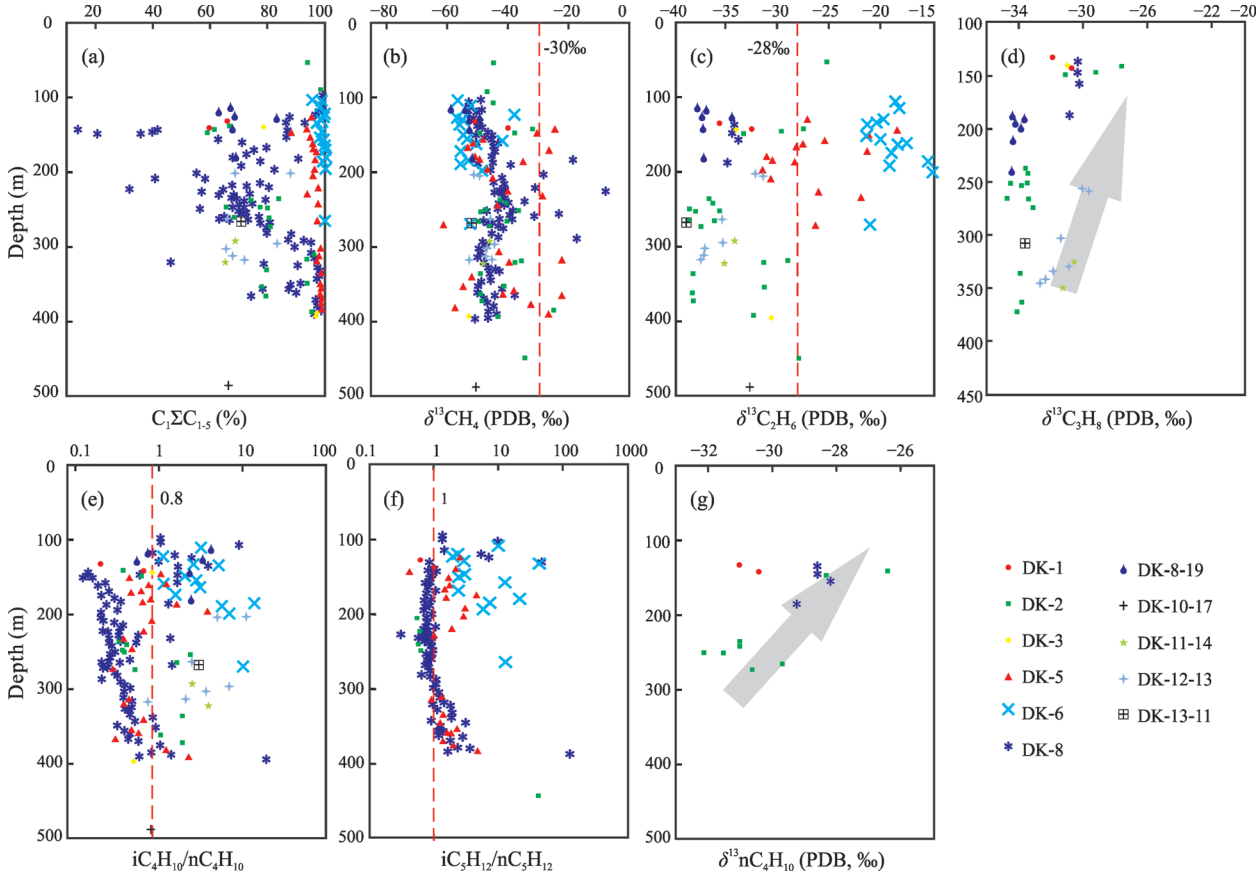

Fig. 5. Gas molecular composition and carbon isotope characteristics with the depth of alkanes gas from gas hydrate and free gas in the Qilian permafrost.

natural gas during the generation process. Natural gas produced by humic organic matter will be much richer in methane content than that produced by sapropelic organic matter (Rice, 1983; Hunt, 1996). Oil and wet gas from sapropelic organic matter in the mature stage would crack into methane at the high to over-mature stage (Rice, 1983). Therefore, the drying coefficient increases as humic organic matter contribution and maturity increase. The genetic type transformed from sapropelic organic matter in the upper part (Upper Middle Jurassic dark mudstone and oil shale) to humic organic matter in the lower part (Upper Triassic Galedesi Fm. and Lower Jurassic coal seams and dark mudstone). At the same time, as depth and thermal maturity increased, the drying coefficient of alkane gas from gas hydrate and free gas was mainly affected by natural gas generation. The trend that drying coefficient increased with depth (Fig. 5a) suggests that it was probably controlled by the thermal maturity and genetic type of organic matter.

4.2 Stable carbon isotope composition of natural gases

As shown in Fig. 6, the $\delta^{13}C_1$ values range from −60.68‰ to −7.87‰, mainly concentrated between −55‰ and −35‰; $\delta^{13}C_2$ values range from −38.40‰ to −15.54‰, mainly concentrated between −38‰ and −18‰, with an average value of −30.36‰. The $\delta^{13}C_3$ values range from −34.70% to −21.20‰, mainly concentrated between −35‰ and −30‰, with an average value of −29.91‰. The $\delta^{13}n$ C_4 values range from −32.1‰ to −26.4 ‰, mainly concentrated between −31 ‰ and −28 ‰, with an average value of −31.94 ‰.

The carbon isotope range of alkane gas decreases with increasing number of carbons (Fig. 6): those for methane, ethane, propane, and butane are 52.81‰, 22.86‰, 13.7‰ and 5.7‰, respectively. The carbon isotope value of n-alkanes increases with increasing carbon number ($\delta^{13}C_1<\delta^{13}C_2<\delta^{13}C_3<\delta^{13}C_4$), which is known as a positive carbon isotope series (James, 1983; Chung et al., 1988; Xia and Gao, 2017). Carbon isotope reversal is caused by different types of natural gas in different thermal maturities, secondary transformation, mixing of two or more kinds of natural gas and high maturity (Burruss and Laughrey, 2010; Zumberge et al., 2012; Tilley and Muehlenbachs, 2013). Most samples have positive carbon isotope sequences ($\delta^{13}C_1<\delta^{13}C_2<\delta^{13}C_3$), and only one sample shows carbon isotope reversal ($\delta^{13}C_1<\delta^{13}C_2>\delta^{13}C_3$). This indicates that the alkane gases of gas hydrate in the study area are mainly related to a thermal origin, and some might have resulted from the mixing of different thermal maturities or secondary transformation.

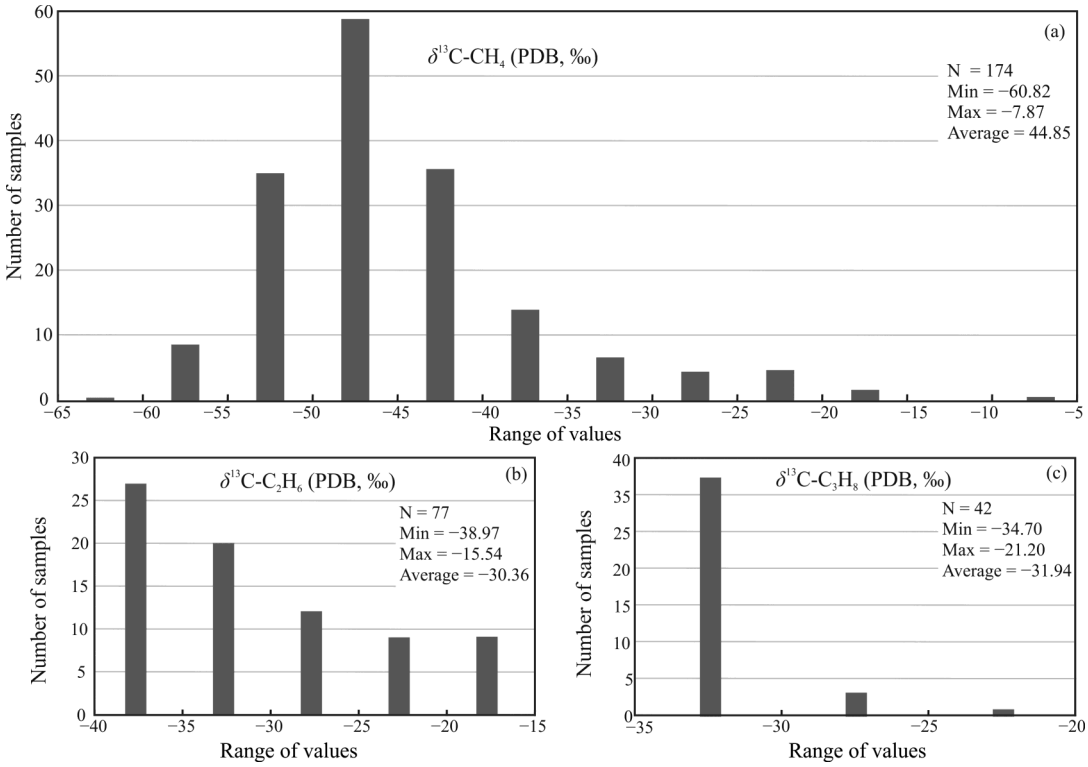

Fig. 6. Carbon isotope frequency distribution of alkanes gas from gas hydrate in the Qilian permafrost.

5 Discussion

5.1 Genetic type of alkane gases

Previous studies have demonstrated that the genetic types of alkane gas can be distinguished by their molecular compositions and carbon isotope values (Dai, 2011; Milkov and Etiope, 2018). Generally, the $\delta^{13}C_1$ value of organic alkane gas is lower than −30‰ (Dai, 1992). In the Qilian permafrost, most samples also show $\delta^{13}C_1$ values lower than −30‰ (Fig. 7a), and only a small part of the $\delta^{13}C_1$ values from boreholes DK-5 and DK-8 was greater than −30‰ (Fig. 5b). Therefore, the alkane gases of the Qilian permafrost are organic origin.

Genetic types of the natural gas have been divided into organic gas and inorganic gas (Milkov and Etiope, 2018) (Fig. 7a). Most of our samples fall into the thermogenic area and the intersection between the organic and inorganic genesis area. Therefore, alkane gases of the study area are of organic origin, with no obvious inorganic contribution. Furthermore, as seen in the $\delta^{13}CH_4$–$\delta^{13}CO_2$ plot (Fig. 7b), most of the samples fall in the area of thermogenic and the intersection of thermogenic and abiotic origin, and only three samples from boreholes DK-2, DK-3 and DK-8 fall in the secondary biodegradable area. Combined with the positive carbon isotope series, we infer that the alkane gases are predominately thermogenic, and the biological gas was the product of secondary action, which is in accordance with the results of the thermogenic gas seen in Fig. 7a. Then biodegradation slightly changed the composition and $\delta^{13}C$ values of the alkane gases in the Qilian permafrost. In summary, alkane gases of the gas hydrates in the study area are mainly of thermogenic origination.

Moreover, thermogenic natural gas can be further subdivided into coal-type gas and oil-type gas (Dai et al., 1985; Dai, 1992; Liu et al., 2019). Commonly, the $\delta^{13}C$ value of coal-type gas is higher than that of oil-type gas. Compared with methane and propane, carbon isotopes of ethane experience fewer secondary changes after the formation of natural gas (Peters et al., 2005). Therefore, carbon isotopes of ethane are more accurate indicators that can reflect the relationship between the genetic type of source rocks and natural gas. The discriminating value used for ethane carbon isotopes is −28‰: $\delta^{13}C_2H_6 <$ −28‰ indicates an oil-type gas; $\delta^{13}C_2H_6 >$ −28‰ indicates a coal-type gas (Dai, 1992, 2011; Liu et al., 2008, 2019). In the Qilian permafrost, most $\delta^{13}C_2H_6$ values of alkane gases are less than −28‰, whereas the $\delta^{13}C_2H_6$ values of some samples (DK-2, DK-5, DK-6) are greater than −28‰ (Fig. 5c), indicating that the alkane gases from gas hydrate and free gas in the study area are mainly oil-type gases with a small number of coal-type gases. Furthermore, methane content and methane carbon isotopes have been used to judge the genetic type of natural gas (Dai , 1992). Most alkane gas samples fall in the oil-associated gas area (Fig. 7c), and only a few samples fall in the areas of sub-biogenic gas, oil-cracking gas, coal-derived gas, coal-type gas, and abiogenic gas, which also indicates that the alkane gases are oil-type gases with few coal-type gas, mixed, and biodegradation gases. Therefore, alkane gases from boreholes DK-5 and DK-6 are mainly products of himic organic whereas the others are products of sapropelic organic.

Light hydrocarbons from sapropelic organic matter are

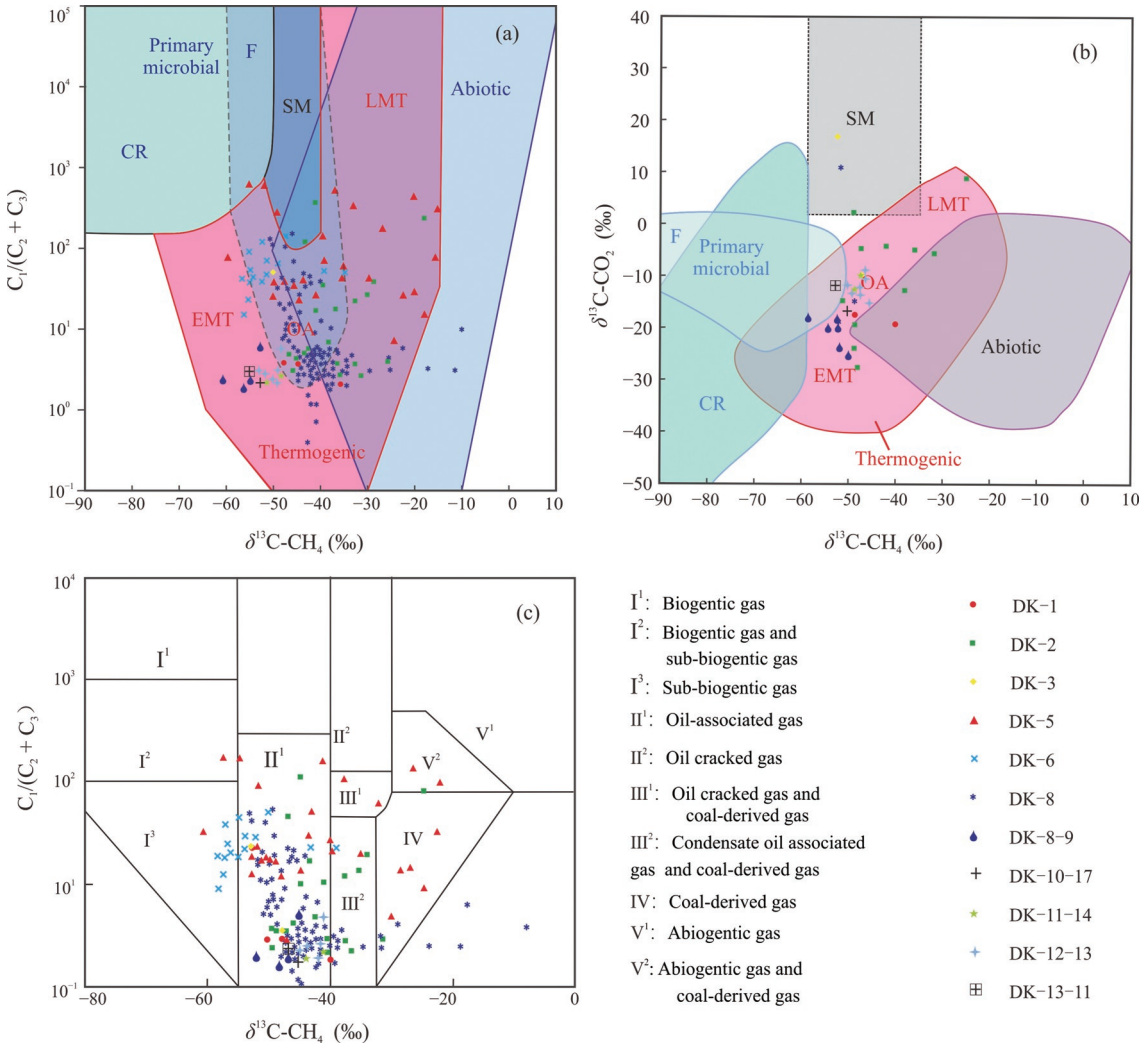

Fig. 7. Genetic diagram of alkanes gas from gas hydrate in the Qilian permafrost.
(a) Genetic diagram of $\delta^{13}C_1$ versus $C_1/(C_2 + C_3)$ (after Milkov and Etiope, 2018); (b) genetic diagrams of $\delta^{13}C_1$ versus $\delta^{13}C\text{-}CO_2$ (after Milkov and Etiope, 2018); (c) plot of $\delta^{13}C_1$ vs. C_1/C_{2+3} of alkanes gas from gas hydrate in the Qilian permafrost (after Dai, 1992). CR, CO_2 reduction; F, methyl-type fermentation; SM, secondary microbial; EMT, early mature thermogenic gas; OA, oil-associated thermogenic gas; LMT, late mature thermogenic gas.

rich in n-heptane (nC_7) and dimethyl cyclopentane ($\Sigma DMCC_5$), whereas hydrocarbons from humic organic matter are rich in methyl cyclohexane (MCC_6). A C_7 light hydrocarbon system trigonometric chart has been used in many studies to identify coal-type gases and oil-type gases (Dai, 1992; Odden et al., 1998; Hu and Zhang, 2011). As seen in the triangular map of these lipids, most liquid light hydrocarbons associated with gas hydrates and free gas fall in the oil-type gas area, and a few fall in the coal-type gas area (Fig. 8). The carbon isotope series and light hydrocarbons associated with alkane gas show multiple origins: Ethane carbon isotopes of the alkane gas associated with light hydrocarbons from DK11-14, DK12-13 and DK13-11 show typical features of oil-type gas. Besides, evidence from light hydrocarbon components suggests that natural gases are coal-type gases and oil-type gases in same boreholes. A reasonable assumption that can explain the multiple origins of alkane gas is that coal-type gases and oil-type gases co-exist at different depths in

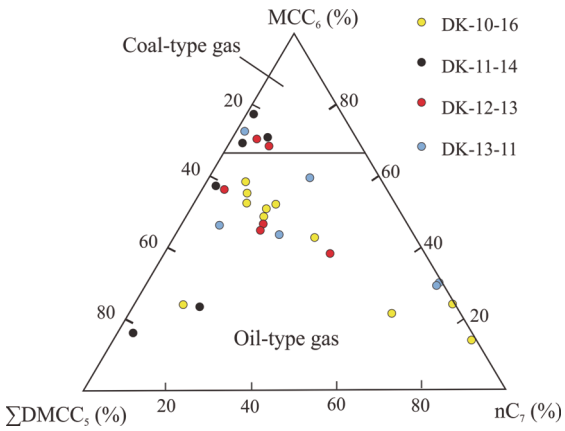

Fig. 8. Identification trigonometric diagram of coal-derived gas and oil-type gas by composition of C_7 light hydrocarbon related to alkanes gas from gas hydrate in the Qilian permafrost (modified from Zhang et al., 2018).

the same borehole rather than a mixture of coal-type gases and oil-type gases. This is likely to occur when the natural gas produced by the source rock is enrichment in situ without migration, and there is no mixture of multiple hydrocarbons. Therefore, alkane gases from gas hydrates and free gases in the Qilian permafrost are mainly oil-type gases with partial coal-type gases.

5.2 Biodegradation of alkane gases

Sensitivity of hydrocarbons to biodegradation depends on the size of the molecule and the structure of the carbon chain (Peter et al., 2005). In general, n-alkanes are more susceptible to microbial degradation than iso-alkanes (Katz et al., 2002; Boreham et al., 2008). Thus, the ratio of branched-chain alkane to straight-chain paraffin is an important indicator to identify whether biodegradation of natural gas has occurred. At the same time, the $\delta^{12}C$ molecules in high-carbon alkanes are preferentially decomposed into low-carbon alkanes, resulting in more positive values of the $\delta^{13}C_3$ and negative values of $\delta^{13}C_1$ for residual oxidized components (Milkov, 2011). Therefore, iC_4/nC_4, iC_5/nC_5, $\delta^{13}C_3$, $\delta^{13}nC_4$ are important indicators for discriminating biodegradation. As seen in Fig. 5e, ratios of iC_4/nC_4 from different boreholes are higher than 0.8, with maximum value up to 18.41. Meanwhile, iC_5/nC_5 ratios in boreholes DK-5, DK-6, DK-8 vary widely (Fig. 5f), indicating that the alkane gas underwent biodegradation more or less. Generally, the scale of the biodegradation increases with decreasing burial depth. With the burial depth decreasing, the values of $\delta^{13}C_3$ and $\delta^{13}nC_4$ in many boreholes increase from −35‰ to −28‰ and −32‰ to −26‰, respectively (Fig. 5d, g), further confirming that the alkane gases underwent biodegradation.

Propane is consumed preferentially during biodegradation, resulting in a sharp reduction of content. As a result of biodegradation, C_2/iC_4 ratios of natural gases are constant while C_2/C_3 ratios increase rapidly, which differs significantly from thermogenic gases (Prinzhofer and Battani, 2003). As seen in Fig. 9, many samples with large C_2/C_3 ratios and small C_2/iC_4 ratios from boreholes DK2, DK5, DK6, DK 8 imply that part of the alkane gases is biodegraded. Previous studies have shown that the $\delta^{13}C_1$ value of the biodegradation is in the range of −60 ‰ to −35 ‰, and $\delta^{13}C\text{-}CO_2$ is higher than 2 ‰ (Milkov, 2011; Milkov and Etiope, 2018). In our study, three samples are in the secondary microbial area (Fig 7b).

In summary, multiple lines of evidence from molecular compositions and carbon isotopes reveal biodegradation for the alkane gas of all the boreholes in the Qilian permafrost.

5.3 Thermal maturity of alkane gases

The methane carbon isotopic compositions of hydrocarbon gas are usually inherited from the source-derived kerogen (Schoell, 1983; James, 1990). In addition, many theoretical and experimental studies have shown that $\delta^{13}C_1$ values in alkane gas are also strongly controlled by thermal maturity (Waples and Tornheim, 1978; Chung et al., 1988; Clayton, 1991; Rooney et al., 1995; Berner and Faber, 1996). Hydrocarbon gases are formed through the fracturing of carbon-carbon bonds in complex kerogen

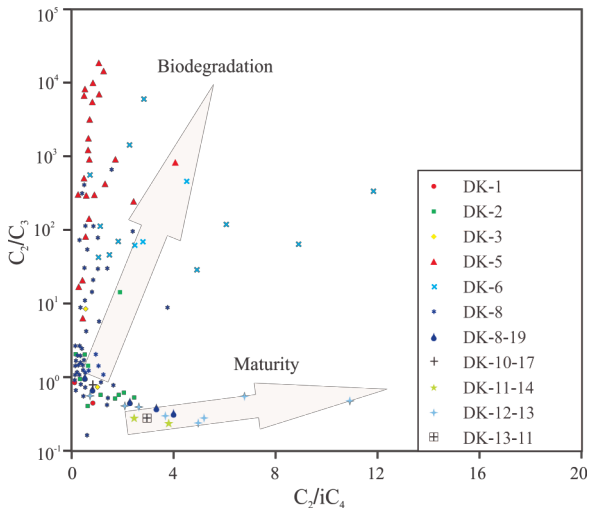

Fig. 9. Correlation diagrams between the C_2/C_3 and C_2/iC_4 values of alkanes gas from gas hydrate in the Qilian permafrost (after Prinzhofer and Battani, 2003).

molecules or liquid oils (Chung et al., 1988; Clayton, 1991; Rooney et al., 1995). Based on the correlation that methane carbon isotopes become heavier with thermal maturity, Berner and Faber (1996) used methane and ethane carbon isotopes with different kerogen types to estimate the maturity of natural gas formation (Fig. 10). In this study, we also used the method to evaluate thermal maturity of the alkane gas in the Qilian permafrost. Some samples from gas hydrates and free gas are consistent with type II kerogen and type III kerogen curves and most samples are located near the type II curve (Fig. 10), demonstrating that the vitrinite reflectance (V*R*o) values for alkane gases are mainly less than 1.1%. A part of the samples from boreholes DK-5 and DK-6 are located far away from the type II, III kerogen curves, and their *R*o values are between 1.6% and 2.0 %, indicating probably higher thermal maturity of the natural gas from the two boreholes. The result is consistent with the high thermal maturity shown in Fig 7a.

The carbon isotope differential values of n-alkanes in natural gases decrease with increasing thermal maturity, but would not decrease with genetic type or whether mixed with other gases (James, 1983). Therefore, *R*o estimation does not require prior understanding of the genetic type of natural gas (James, 1990; Boreham et al., 2001). As shown in Fig. 11, although samples of alkane gases are somewhat dispersed, most are mainly distributed near the theoretical line with the estimated *R*o values around 0.6% ~ 1.8%, mainly between 0.55% and 1.2%. Overall, the thermal maturity for the same samples seen in Fig. 10 is lower than that shown in Fig. 11, which is mainly due to the light carbon isotopes of methane caused by biodegradation. Although differences exist in (*R*o) values of the alkane gas from different methods, there is a clear two-stage distribution for the thermal maturity. Most *R*o values fall in the range of 0.6%−1.2%, with a maturity stage, and some part of the *R*o values, distributed in boreholes DK-5 and DK-6, greater than 1.2%, i.e., a high maturity stage.

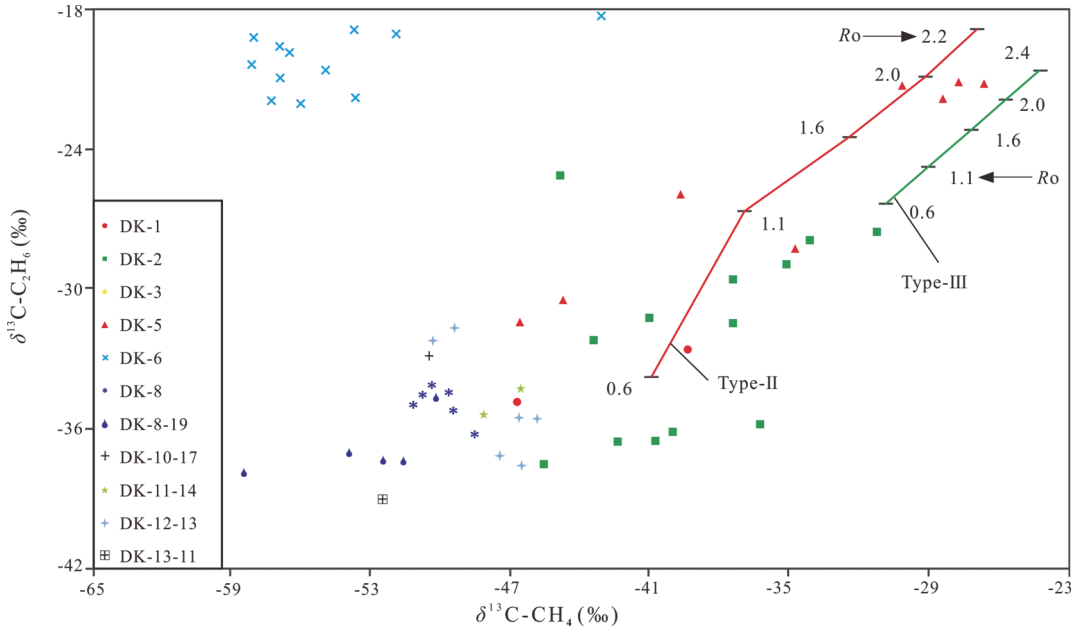

Fig. 10. Vitrinite reflectance (V*R*o) curves for type II and type III kerogens were shifted in line with average $\delta^{13}C$ values of −24.6‰ for type II kerogen and −23.8‰ for type III kerogen from a previous study (after Greene et al., 2004).

5.4 Primary and secondary cracking

According to traditional hydrocarbon generation theory, a large amount of natural gases and a small amount of oil are produced from thermal cracking of humic organic matter. Before the formation of liquid hydrocarbon as the primary product, a small amount of natural gas can be generated directly from sapropelic organic matter (Behar et al., 1995; Lorant et al., 1998). The cracking of liquid hydrocarbon coexisting with kerogen occurs in the high thermal maturity stage, and the degree of thermal cracking of crude oil is much higher than that of kerogen (Tissot and Welte, 1984). Therefore, the sapropelic organic matter can produce oil-type gases in two ways (James, 1990; Behar et al., 1995; Lorant et al., 1998; Prinzhofer et al., 2000; Tang et al., 2000; Prinzhofer and Battani, 2003): (1) direct cracking of kerogen; (2) oil cracking gas produced by the thermal cracking of crude oil. Diagrams of $\delta^{13}C_2 - \delta^{13}C_3$ versus C_2/C_3 can be used to distinguish kerogen cracking gas from crude oil cracking gas (Lorant et al., 1998). A few thermal original samples (relatively small C_2/C_3, with values ranging from 0 to 8) are distinguished as secondary cracking of oil and cracking of kerogen (Fig.

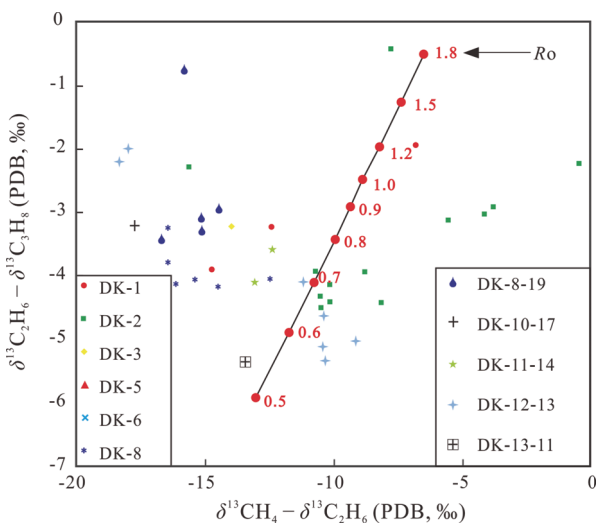

Fig. 11. Cross plot of $\delta^{13}C_1 - \delta^{13}C_2$ versus $\delta^{13}C_2 - \delta^{13}C_3$ showing the maturity of alkanes gas from gas hydrate in the Qilian permafrost. The red numbers refer to VRo (James, 1983).

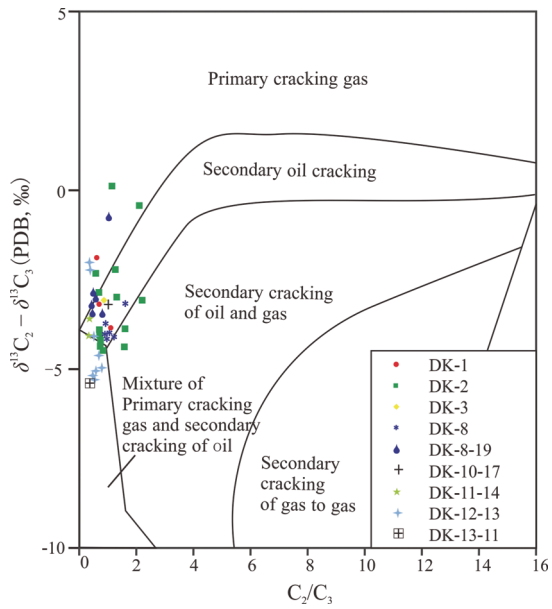

Fig. 12. Diagram showing C_2/C_3 versus $\delta^{13}C_2 - \delta^{13}C_3$ for identification of kerogen-cracking gas and oil-cracking gas at different thermal evolutionary stages of alkanes gas from gas hydrate in the Qilian permafrost (after Lorant et al., 1998).

12): (1) some located in the kerogen cracking gas area; (2) many samples fall in the area of secondary cracking oil, with a small number located in the area of secondary cracking oil or gas, and the area of mixed primary cracking gas and secondary cracking oil gas. Thus, the alkane gases from these samples are primary from secondary cracking oil, which are composed of some kerogen cracking gas and crude oil cracking wet gas to dry gas. *R*o values range from 1.6% to 3.2%, at the stage of cracking crude oil, in which natural gas can be produced (Li et al., 2018). The minimum *R*o value from boreholes DK-5 and DK-6 is higher than 1.2%, indicating that the natural gases were probably generated from the two hydrocarbon generation methods (i.e., direct cracking of kerogen and cracking of crude oil and wet gas). According to the thermal maturity, alkane gases from gas hydrates are also composed mainly of secondary cracking gases, including crude oil cracking gas and secondary wet gas cracking to produce dry gas.

5.5 Gas-source correlation

5.5.1 Origins of alkane gases

As noted above, there are two source rocks in the Qilian permafrost region, the Galedesi Fm. and the Yaojie Fm. (Hao et al., 2016, 2017). The Jurassic Yaojie Fm. source rocks are composed of oil shales, mudstones, carbonaceous mudstones, and coal seams from top to bottom. The organic matter also shows types I-II kerogen and III kerogen. The *R*o values of samples range from 0.96% to 1.8%, representing a mature stage. Dark mudstones mainly occur in the Triassic Galedesi Fm., of which the organic matter is type II_2 to III and *R*o values higher than 1.2% (Fan et al., 2020). The organic abundance of these two source rocks is relatively high, indicating that both source rocks have good hydrocarbon generation capacity (Gong et al., 2014). The profile of the source rocks shows that the genetic type of the upper Yaojie Fm. mudstones and oil shales is sapropelic organic matter, while the genetic type of the lower Yaojie Fm. and Galedesi Fm. coal seams and mudstones is humic organic matter.

Based on oil and gas generation models (Tissot and Welte, 1984; Dai, 1992), at the oil generation window (0.6% < *R*o < 1.3%) of sapropelic organic matter, much liquid hydrocarbon associated with some wet gas are produced (Fig. 13a). As thermal maturity increases (*R*o> 1.3%), less liquid hydrocarbons and heavy gaseous hydrocarbons are generated, and a large amount of methane is produced. By contrast, little light oils and wet gases are generated by humic organic matter in the mature stage (0.6% < *R*o < 1.3%). When the thermal maturity increases (*R*o > 1.3%), copious dry gases are formed by the continuous cracking of the generated wet gases and oils, constituting the whole process of primarily natural gas generation (Fig. 13b).

The alkane gases from gas hydrates and free gas in the Qilian permafrost include wet gas and dry gas. The dry gas distributed in DK-5 and DK-6 are mainly formed at a high-over mature stage, with genetic types that are mainly microbial and type III kerogen. This is closely related to the genetic type and thermal maturity of the organic matter from the Upper Triassic Galedisi Fm., quite different to the Jurassic source rocks. Combined with the hydrocarbon generation model of humic kerogen, the organic matter of the Galedsi Fm. in the study area is in the high mature stage, which can produce dry gas directly, and it also explains well how the two borehole alkane gases are mainly dry gas. This hydrocarbon generation model explains reasonably that the dry gas in the study area is mainly produced by humic organic matter in the Galedesi Fm. at high maturity.

In contrast, wet gases are mainly distributed in other

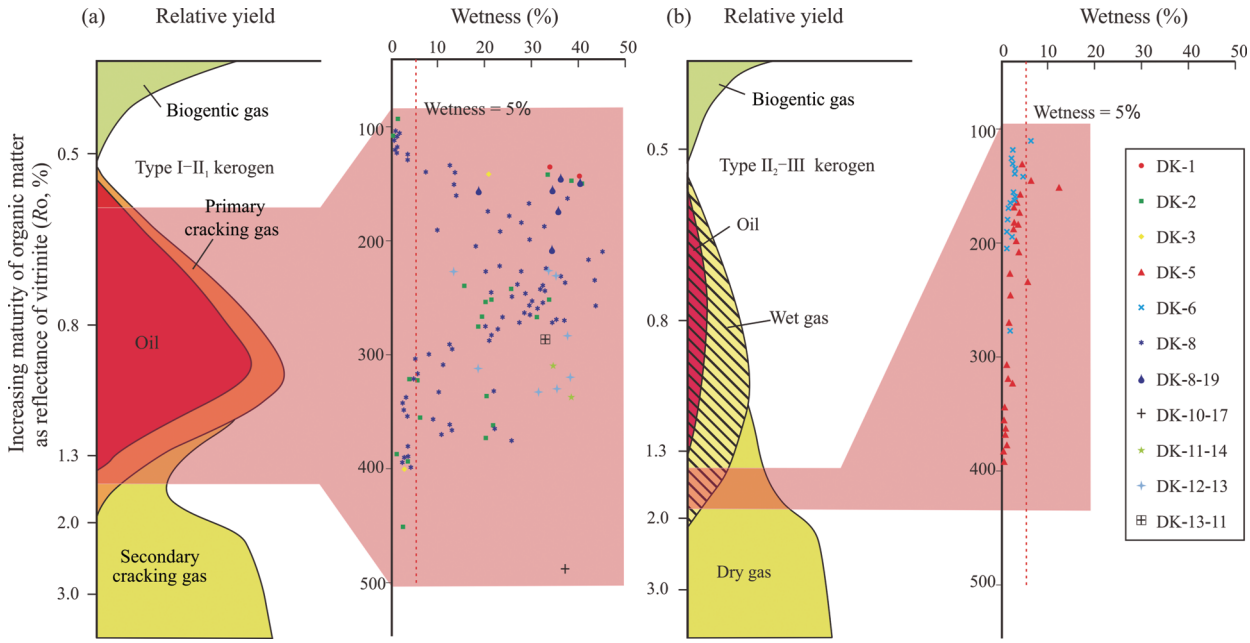

Fig. 13. Conceptual model of gas generation from sapropelic matter (type I and II_1 kerogen) and humic matter (type II_2 and III kerogen and/or coal), and relationship between wetness and burial depth of natural gas of alkanes gas from gas hydrate in the Qilian permafrost. Diagram modified from Hunt (1979), Tissot and Welte (1984) and Dai (1992).

boreholes with *R*o values ranging from 0.6% to 1.2%, revealing the oil generation window. The wet gases mainly originated from the cracking gases of crude oils, in part from kerogen cracking gases. This is consistent with the genetic type and the thermal maturity of the organic matter in the upper mudstones and oil shales in the Middle Jurassic. According to the hydrocarbon generation model, sapropelic organic matter of Yaojie Fm. in the study area can produce liquid hydrocarbon, heavy alkanes, and methane at a mature stage (0.6% <*R*o< 1.3%), and the products form wet gas. The discovery of bitumen, oils, and wet gases from the Jurassic (Lu, 2013c; Cheng et al., 2017) further confirmed that the wet gas from oil-type gas is produced at the oil generation window. Multiple factors including organic matter type and thermal maturity of organic matter indicate that the oil-type gases originated from mudstones and oil shales in the upper part of the Yaojie Fm. In general, the alkane gases from the gas hydrates mainly come from the upper part of the Lower Jurassic Yaojie Fm., and partly from the dark mudstones in the Upper Triassic Galedesi Fm.

5.5.2 Origins of carbon dioxide

As one of the most common non-hydrocarbon components in natural gas, carbon dioxide can be divided into three types according to its origin (Dai et al., 1996), namely: organic gas, inorganic gas and mixed gas. (1) The carbon dioxide content of organic gas is usually less than 15% of total natural gases, and the value of δ^{13}C-CO_2 is lower than −10‰; (2) The carbon dioxide content of inorganic gas is greater than 60% in total natural gases, and the δ^{13}C-CO_2 is higher than −8‰; (3) Coexistence and mixing of organic and inorganic origin gas is characterized by −8‰ < δ^{13}C-CO_2 < −10‰. The organic CO_2 mainly originates from thermal decomposition of organic matters, especially the decarboxylase effect of organic matter through decomposition during deep burial (Tissot and Welte, 1984; Dai et al., 1996), bacterial sulfate reduction (BSR) (Machel, 2001) and thermochemical sulfate reduction (TSR) (Liu et al., 2014). Inorganic CO_2 mainly comes from acidic fluid-dissolved carbonate minerals (Fogler and Scott, 1998), calcined carbonate rocks, and deep crust and mantle (Etiope et al., 2011).

On the basis of a comprehensive study of δ^{13}C-CO_2 from many organic and inorganic gases around the world (Milkov and Etiope, 2018), Dai et al. (1996) proposed an identification map for the organic and inorganic origins of carbon dioxide (Fig. 14). Most of the carbon dioxide contents in the decomposition from gas hydrates and free gases are less than 10%, with δ^{13}C-CO_2 values less than −10 ‰, which fall in the organic origin region. The δ^{13}C-CO_2 values of two samples are between −10 ‰ and −8 ‰, and their carbon dioxide contents are less than 10%, falling into the region of both organic and inorganic origins. The carbon dioxide content of one sample is higher than 10%, with δ^{13}C-CO_2 values located between −10 ‰ and −8 ‰, falling into the mixed region of organic and inorganic origin. The δ^{13}C-CO_2 value of only one sample from borehole DK-2 is higher than −8 ‰, falling into the inorganic genetic region. In summary, the carbon dioxide contents of decomposing gases from gas hydrates

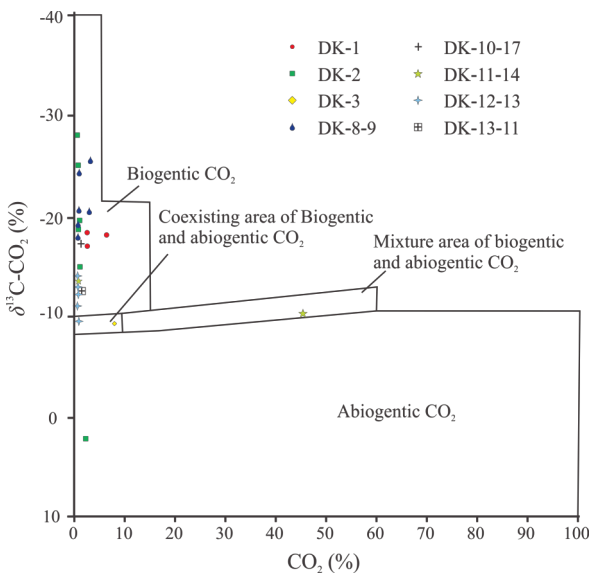

Fig. 14. Geochemical characteristics of CO_2 from alkanes gas from gas hydrate in the Qilian permafrost (Dai et al., 1996).

and free gases are less than 10%, representative of an organic origin. Anaerobic biodegradable natural gases caused the increase of n-alkanes δ^{13}C. The n-alkanes are oxidized into H_2 and CO_2, and the resulted δ^{13}C value of the CO_2 is up to 2.3‰, which can explain the high isotope values from borehole DK2 and the only sample of inorganic genesis.

Microbial BSR generally occurs when the temperature is less than 80°C and the *R*o value is 0.2%~0.3% (Machel, 2001). The alkane gases of the gas hydrates in the Qilian permafrost area are produced at the high maturity stage, and the *R*o value is much greater than 0.3%. Thus, the decomposition gases of the gas hydrates are not generated by BSR. Thermochemical sulfate reduction (TSR) is a chemical reaction of sulfate under the action of high temperature chemical reduction with organic matter, and the natural gas produced by it has a high hydrogen sulfide concentration. There are no obvious hydrogen sulfide gases within the gases of gas hydrates and free gases in the area, which negates the fact that carbon dioxide is produced by the TSR reaction in the study area. Therefore, carbon dioxides from gas hydrates and free gases are not the products from BSR and TSR. The carbon isotope values of carbon dioxide produced by thermal decomposition of organic matter ranges from −39 ‰ to −10 ‰ (Dai et al., 1996). The carbon isotope values of carbon dioxide from gas hydrates and free gases in the Qilian permafrost are consistent with that of thermal decomposition of organic matter, indicating that the carbon dioxide mainly generated by the thermal decomposition of organic matter in the area. Composition of gases formed by petroleum and condensate oil is $4CO_2 \bullet 46CH_4 \bullet N_2 \bullet H_2S$ + trace hydrogen in the mature-over-mature stage (Aksenov and Anisimot, 1982). According to the combined gas molecular formulas, the carbon dioxide content accounts for ~7.7% of the total natural gases, meaning that the CO_2 content of the thermal

decomposition of organic matter is less than 8%. Most of the CO_2 content in the study area is less than 8%, further proving that the CO_2 in the natural gases from gas hydrates might have been an associated production of organic matter thermal decomposition.

6 Conclusions

The molecular and stable carbon isotopic compositions of natural gas samples from gas hydrates and free gases in the Qilian permafrost were analyzed with the aim of exploring their genetic type, thermal maturity, and origin. The following salient conclusions can be drawn from this study:

(1) Natural gases are mainly composed of abundant alkane gases and a small amount of CO_2 and N_2. The alkane gases are mainly oil-type gases with a small amount of coal-type gases. Oil-type gases originate from mudstones and oil shales in the upper part of the Lower Jurassic. Coal-type gases originate from mudstones of the Lower Jurassic and Upper Triassic.

(2) Most of the alkane gases are thermogenic gases generated at a thermal stage with *R*o ranging from 0.6% to 1.5%, suggesting that they are mainly composed of crude oil-cracking gases with some primary cracking gases and wet gas cracking gases. Other alkane gases at a thermal stage have *R*o values higher than 1.2%, reflecting the direct generation of gas from kerogen. Generation of alkane gases is mainly controlled by secondary cracking with minor contributions from primary cracking.

(3) Microbial alteration of hydrocarbon gases has been observed in the Lower Jurassic Yaojie Fm., with secondary biogenic gases in the study area recognized for the first time.

(4) CO_2 with abundance less than 10% is organic, the origination of which is mainly derived from organic matter decomposition, and a small amount CO_2 came from biodegradation.

(5) The Upper Triassic Galedesi Fm. of the Muli sag has considerable potential for deep gas exploration. The distribution of the gases is primarily controlled by kerogen type and thermal maturity of the source rocks as well as the activity of the source-rock connecting faults.

Acknowledgments

This work was granted by the National Natural Science Foundation of China (Grant nos. 41702144; 41802212), the State Key Laboratory of Organic Geochemistry, GIGCAS (Grant no. SKLOG-201908), and the Fundamental Research Funds for the Central Universities (Grant no. 2652018234). The authors would like to thank the Qinghai Coal Geology 105 Exploration Team for kindly providing part of the data in this study. Kang Huiling and Susan Turner (Brisbane) are thanked for their help with English language of this manuscript. We also want to thank anonymous manuscript reviewers for their constructive suggestions and comments which significantly improved the quality of this manuscript.

Manuscript received May 15, 2019
accepted Jun. 4, 2020
associate EIC: XU Tianfu
edited by GUO Xianqing

References

Aksenov, A., and Anisimot, L., 1982. Forecast of the sulphide distribution in subsalt sediments within the Caspian Depression. Social Geology, 10: 46–52.

Behar, F., Vandenbroucke, M., Teermann, S.C., Hatcher, P.G., Leblond, C., and Lerat, O., 1995. Experimental simulation of gas generation from coals and a marine kerogen. Chemical Geology, 126: 247–260.

Berner, U., and Faber, E., 1996. Empirical carbon isotope/maturity relationships for gases from algal kerogens and terrigenous organic matter, based on dry, open-system pyrolysis. Organic Geochemistry, 24(10): 947–955.

Boreham, C.J., Hope, J.M., and Hartung, K.B., 2001. Understanding source, distribution, and preservation of Australian natural gas: A geochemical perspective. Appea Journal, 41(1): 523–547.

Boreham, C.J., Edwards, D.S., Hope, J., Chen, J., and Hong, Z., 2008. Carbon and hydrogen isotopes of neo-pentane for biodegraded natural gas correlation. Organic Geochemistry, 39(10): 1483–1486.

Burruss, R.C., and Laughrey, C.D., 2010. Carbon and hydrogen isotopic reversals in deep basin gas: Evidence for limits to the stability of hydrocarbons. Organic Geochemistry, 41(12): 1285–1296.

Cao, D.Y., Wang, D., Li, J., and Dou, X.Q., 2012. Gas source analysis of natural gas hydrate of Muri coalfield in Qilian Mountain permafrost, Qinghai Province, China. Journal of China coal Society, 37(8): 1364–1368 (in Chinese with English abstract).

Cheng, B., Xu, J.B., Lu, Z.Q., Li, Y.H., Wang, W.C., Yang, S., Liu, H., Wang, T., and Liao, Z.W, 2017. Hydrocarbon source for oil and gas indication associated with gas hydrate and its significance in the Qilian Mountain permafrost, Qinghai, Northwest China. Marine and Petroleum Geology, 89: 20–215.

Cheng, Q.S., Gong, J.M., Zhang, M., Wang, W.C., Cheng, W.J., Jiang, Y.B., Jiang, Y.B., Xu, C.F., Cheng, Z.Q., and Tian, R.C., 2016. Geochemical characteristics of hydrocarbon source rocks in the qilian mountain permafrost and gas sources for gas hydrate. Marine Geology & Quaternary Geology, 36(5): 139–147 (in Chinese with English abstract).

Chung, H.M., Gormly, J.R., and Squires, R.M., 1988. Origin of gaseous hydrocarbons in subsurface environments: Theoretical considerations of carbon isotope distribution. Chemical Geology, 71(1): 97–104.

Clayton, C., 1991. Carbon isotope fractionation during natural gas generation from kerogen. Marine and Petroleum Geology, 8(2): 232–240.

Collett, T., Johnson, A., Knapp, C., and Boswell, R., 2010. Natural gas hydrates — Energy resource potential and associated geologic hazards. AAPG Memoir, 89.

Dai, J.X., 1992. Identification of various alkane gases. Science in China, 35(10): 1246–1257 (in Chinese).

Dai, J.X., 2011. Significance of the study on carbon isotopes of alkane gases. Natural Gas Industry, 31(12): 1–6 (in Chinese with English abstract).

Dai, J.X., Ni, Y.Y., Huang, S.P., Peng, W.L., Han, W.X., Gong D.Y., and Wei W., 2017. Genetic types of gas hydrates in China. Petroleum Exploration and Development, 44(6): 887–898.

Dai, J.X., Qi, H.F., and Song, Y., 1985. Primary discussion of some parameters for identification of coal-and oil-type gases. Acta Petroleum Sinica, 6: 31–38 (in Chinese with English abstract).

Dai, J.X., Song, Y., Dai, C.S., and Wang, D.R., 1996. Geochemistry and accumulation of carbon dioxide gases in China. AAPG Bulletin, 80(10): 1615–1626.

Etiope, G., Baciu, C., and Schoell, M., 2011. Extreme methane deuterium, nitrogen, and helium enrichment in natural gas from the Homorod seep (Romania). Chemical Geology, 280(1

–2): 89–96.
Fan, D.W., Lu, Z.Q., Li, G.Z., Xiao, R., 2020. Organic geochemical characteristics of the Carboniferous–Jurassic potential source rocks for natural gas hydrates in the Muli Depression, Southern Qilian Basin. Oil & Gas Geology, 41(2): 348–358 (in Chinese with English abstract).
Fogler, C., and Scott, N.F., 1998. The kinetics of calcite dissolution in acetic acid solutions. Chemical Engineering Science, 53(22): 3863–3874.
Greene, T.J., Zinniker, D., Moldowan, J.M., Keming, C. and Aiguo, S., 2004. Controls of oil family distribution and composition in nonmarine petroleum systems: a case study from the turpan-hami basin, northwestern china. AAPG Bulletin, 88: 447–481.
Hao, A.S., Wang, R., Li, J., Tian, B.Z., Shi, J.L., Li, X.L., Cui, J.F., and Lv, M.L., 2017. Evaluation and petroleum exploration potential of hydrocarbon source rocks in the Muli depression, southern Qilian basin, Bulletin of Mineralogy Petrology and Geochemistry, 36(1): 134–140 (in Chinese with English abstract).
Hao, A.S., Li, J., Wang, D.L., Li, Z.S., Cui, J.F., Cui, H.Y., and Jiang, X.H., 2016. Biomarker characteristics of source rock of carboniferous and upper Triassic Galedesi Formation in southern Qilian basin. Unconventional Oil Gas, 3(1): 7–13 (in Chinese with English abstract).
He, X.L., Liu, C.L., Meng, Q.G., Lu, Z.Q., Wen, H.J., Li, Y.H., Zhang, S.L., and Wang, J.T., 2015. Gas composition of hydrate-bearing cores in Juhugeng Drilling Area in Qinghai and its indicative significance. Geoscience. 29(5): 1194–1200 (in Chinese with English abstract).
Hu, G.Y., and Zhang, S.C., 2011. Characterization of low molecular weight hydrocarbons in Jingbian gas field and its application to gas sources identification. Energy Exploration & Exploitation, 29(6): 777–796.
Huang, D.F., Liu, B.Q., Wang, T.D., Xu, Y.C., Chen, S.J., and Zhao, M.J., 1999. Genetic type, and maturity of Lower Paleozoic marine hydrocarbon gases in the eastern Tarim Basin. Chemical Geology, 162 (1): 65–77.
Huang, X., Liu, H., Zhang, J.Z., Wang, P.K., Xiao, R., Pang, S.J, Zhang, S., and Zhu, Y.H., 2016. Genetic-type and its significance of hydrocarbon gases from permafrost-associated gas hydrate in Qilian Mountain. Chinese Journal of Geology, 51(3): 934–945 (in Chinese with English abstract)
Huang, X., Zhu, Y.H., Wang, P.K., and Guo, X.W., 2011. Hydrocarbon gas composition and origin of core gas from the gas hydrate reservoir in Qilian mountain permafrost. Geological Bulletin of China, 30(12): 1851–1856 (in Chinese with English abstract).
Hunt, J.M., 1979. Petroleum Geochemistry and Geology. Freeman W. H., San Francisco.
Hunt, J.M., 1996. Petroleum Geochemistry and Geology. W.H. Freeman: San Francisco.
James, A.T. 1983. Correlation of natural gas by use of carbon isotopic distribution between hydrocarbon components. AAPG Bulletin, 74 (7): 1176–1191.
James, A.T., 1990. Correlation of reservoir gases using the carbon isotopic compositions of wet gas components. AAPG Bulletin,74 (9): 1441–1458.
Jenden, P.D., Kaplan, I.R., Poreda, R., and Craig, H., 1988. Origin of nitrogen-rich natural gases in the California Great Valley: Evidence from helium, carbon, and nitrogen isotope ratios. Geochimica et Cosmochimica Acta, 52 (4): 851–861.
Katz, B.J., Narimanov, A., and Huseinzadeh, R., 2002. Significance of microbial processes in gases of the south Caspian basin. Marine and Petroleum Geology, 19(6): 783–796.
Kvenvolden, K.A., 1993. Gas hydrates—Geological perspective and global change. Reviews of Geophysics, 31(2): 173–187.
Kvenvolden, K.A., 1999. Potential effects of gas hydrate on human welfare. Proceedings of the National Academy of Sciences of the United States of America, 96(7): 3420–3426.
Li, J., Zhou, S.X., Gaus, G., Li, Y.J., Ma, Y. Chen, K.F., and Zhang, Y.H., 2018. Characterization of methane adsorption on shale and isolated kerogen from the Sichuan Basin under pressure up to 60 MPa: Experimental results and geological implications. International Journal of Coal Geology, 189: 83–93.
Liu, C.L., He, X.L., Meng, Q.G., Ye, Y.G., Zhu, Y.H., and Lu, Z.Q., 2012. Carbon and hydrogen isotopic compositions characteristics of the released gas from natural gas hydrates in the Qilian Mountain Permafrost. Rock and mineral analysis, 31(3): 489–494 (in Chinese with English abstract).
Liu, L.P., Sun, Z.L., Zhang, L., Wu, N.Y., Yi, C.Q., Jiang, Z.Z., Geng, W., Cao, H., Zhang, X.L., Zhai, B., Xu, C.L., Shen, Z.C. and Jia, Y.G., 2019. Progress in global gas hydrate development and production as a new energy resource. Acta Geologica Sinica (English Edition), 93(3): 231–255.
Liu, Q.Y., Dai, J.X., Li, J., and Zhou, Q.H., 2008. Hydrogen isotope composition of natural gases from the tarim basin and its indication of depositional environments of the source rocks. Science in China, 51(2): 300–311.
Liu, Q.Y., Jin, Z.J., Wu, X.Q., Liu, W.H., Gao, B., Zhang, D.W., Li, J., and Hu, A.P., 2014. Origin and carbon isotope fractionation of CO_2 in marine sour gas reservoirs in the Eastern Sichuan Basin. Organic Geochemistry, 74: 22–32.
Liu, Q.Y., Wu, X.Q., Wang, X.F., Jin, Z.J., Zhu, D.Y., Meng, Q.Q., Huang, S.P., Liu, J.Y., and Fu, Q., 2019. Carbon and hydrogen isotopes of methane, ethane, and propane: A review of genetic identification of natural gas. Earth-Science Reviews. 190: 247–272.
Liu, S.M., Tan, F.R., Huo, T., Tang, S.H., Zhao, W.X, and Chao, H.D., 2020. Origin of the hydrate bound gases in the Juhugeng Sag, Muli Basin, Tibetan Plateau. Journal of Coal Science & Engineering (China), 7(1): 43–57.
Lorant, F., Prinzhofer, A., Behar, F., and Huc, A.Y., 1998. Carbon isotopic and molecular constraints on the formation and the expulsion of thermogenic hydrocarbon gases. Chemical Geology,147: 249–264.
Lu, Z.Q., Tang, S.Q., Luo, X.L., Zhai, G.Y., Fan, D.W., Liu, H., Wang, T., Zhu, Y.H, and Xiao, R., 2020. A natural gas hydrate-oil-gas system in the Qilian Mountain permafrost area, northeast of Qinghai-Tibet Plateau. China Geology, 3(4): 511–523.
Lu, Z.Q., Xue, X. H., Liao, Z. W., and Liu, H., 2013a. Source rocks for gases from gas hydrate and their burial depth in the Qilian mountain permafrost, Qinghai: Results from thermal stimulation. Energy & Fuels, 27(12): 7233–7244.
Lu, Z.Q., Zhu, Y.H., Zhang, Y.Q., Wen, H.J., Li, Y., Jia, Z.Y., Wang, P.K., and Li, Q.H., 2010. Study on genesis of gases from gas hydrate in the Qilian Mountain permafrost, Qinghai. Geoscience, 24(3): 581–588 (in Chinese with English abstract).
Lu, Z.Q., Zhu, Y.H., Liu, H., Zhang, Y.Q., Jin, C., Huang, X., and Wang P.K., 2013b. Gas source for gas hydrate and its significance in the Qilian mountain permafrost, Qinghai. Marine and Petroleum Geology, 43: 341–348.
Lu, Z.Q., Zhu, Y.Q., Liu, H., Zhang, Y.Q., Wang, P.K., and Huang X., 2013c. Oil and gas indications at gas hydrate-bearing intervals in the Qilian Mountain Permafrost. Geoscience, 27(1): 231–238 (in Chinese with English abstract).
Ma, L., Zhang, X., and Li, J., 1999. Experimental investigation on variation of geochemical compositions of natural gas during diffusion under stratigraphic condition. Petroleum Exploration and Development, 20(1): 65–68 (in Chinese with English abstract).
Machel, H.G. 2001. Bacterial and thermochemical sulfate reduction in diagenetic settings—Old and new insights. Sedimentary Geology,140 (1): 143–175.
Makogon, Y.F., 2010. Natural gas hydrates—A promising source of energy. Journal of Natural Gas Science and Engineering, 2 (1): 49–59.
Makogon, Y.F., Holditch, S.A., and Makogon, T.Y., 2007. Natural gas-hydrates—A potential energy source for the 21st Century. Journal of Petroleum Science and Engineering, 56: 14–31.
Milkov, A.V., 2011. Worldwide distribution and significance of secondary microbial methane formed during petroleum biodegradation in conventional reservoirs. Organic Geochemistry, 42: 184–207.

Milkov, A.V., and Etiope G., 2018. Revised genetic diagrams for natural gases based on a global dataset of >20,000 samples. Organic Geochemistry,125: 109–120.

Odden, W., Patience, R. L., and Graas, G., 1998. Application of light hydrocarbons (C_4-C_{13}) to oil/source rock correlations: A study of the light hydrocarbon compositions of source rocks and test fluids from offshore mid-Norway. Organic Geochemistry, 28(12): 823–847.

Peters, K.E., Walters C.C., and Moldowan, J.M., 2005. The Biomarker Guides. Cambridge: Cambridge University Press.

Prinzhofer, A., and Battani, A., 2003. Gas isotopes tracing: An important tool for hydrocarbons exploration. Oil Gas Sci. Technol. Rev. IFP, 58: 299–311.

Prinzhofer, A., Vega, M.A.G., Battani, A., and Escudero, M., 2000. Gas geochemistry of the Macuspana Basin (Mexico): Thermogenic accumulations in sediments impregnated by bacterial gas. Marine and Petroleum Geology, 17: 1029–1040.

Quan, Y.B., Liu, J.Z., Hao, F., Bao, X.H., Xu, S., Teng, C.Y., and Wang, Z.F., 2019. Geochemical characteristics and origins of natural gas in the Zhu III sub-basin, Pearl river mouth Basin, China. Marine and Petroleum Geology, 101: 117–131.

Rice, D., 1983. Relation of natural gas composition to thermal maturity and source rock type in San Juan Basin, Northwestern New Mexico, and Southwestern Colorado. AAPG Bulletin, 67(8): 1199–1218.

Rooney, M.A., Claypool, G.E., and Moses, C.H., 1995. Modeling thermogenic gas generation using carbon isotope ratios of natural gas hydrocarbons. Chemical Geology, 126(3): 219–232.

Schoell, M., 1980. The hydrogen and carbon isotopic composition of methane from natural gases of various origins. Geochimica Et Cosmochimica Acta, 44(5): 649–661.

Schoell, M., 1983. Genetic characterization of natural gases. AAPG Bulletin, 67: 2225–2238.

Sun, L.Y., Wang, X.J., He, M., Jin, J.P., Li, J., Li Y.P., Zhu, Z.Y., and Zhang G.X., 2020. Thermogenic gas controls high saturation gas hydrate distribution in the Pearl River Mouth Basin: Evidence from numerical modeling and seismic anomalies. Ore Geology Reviews, 127(4): 1–16.

Tan, F.R., Liu, S.M., Cui, W.X., Wan, Y.Q., Yang, C., Zhang, G.C, Liu, W.G., Du, F.P., and Fan, Y.H., 2017. Origin of gas hydrate in the Juhugeng mining area of Muli Coalfield. Acta Geologica Sinica, 91(5): 1158–1167 (in Chinese with English abstract).

Tang, Y., Perry, J.K., Jenden, P.D. and Schoell, M., 2000. Mathematical modeling of stable carbon isotope ratios in natural gases. Geochimica et Cosmochimica Acta, 64: 2673–2687.

Tilley, B., and Muehlenbachs, K., 2013. Isotope reversals and universal stages and trends of gas maturation in sealed, self-contained petroleum systems. Chemical Geology, 339:194–204.

Tissot, B.T., and Welte, D.H., 1984. Petroleum Formation and Occurrences. Berlin: Springer.

Wang, P.K., Zhu, Y.H., Lu, Z.Q., Guo, X.W., and Huang, X., 2011. Gas hydrate in the Qilian Mountain permafrost and its distribution characteristics. Geological Bulletin of China, 30 (12): 1839–1850 (in Chinese with English abstract).

Waples, D.W., and Tornheim, L., 1978. Mathematical models for petroleum-forming processes: Carbon isotope fractionation. Geochimica et Cosmochimica Acta, 42 (5): 467–472.

Xia, X., and Gao, Y., 2017. Mechanism of linear covariations between isotopic compositions of natural gaseous hydrocarbons. Organic Geochemistry, 113: 115–123.

Xiao, K., Zou, C.C., Lu, Z.Q., Li, H. X., Qin, Z.L., and Ge, K.P., 2020. The acoustic log method of estimating gas hydrate saturation in gas hydrate reservoirs. Acta Geologica Sinica, 94 (5): 1664–1674 (in Chinese with English abstract).

Xiao, W.J., Windley, B.F., Yong, Y., Yan, Z., Yuan, C., Liu, C., and Li, J., 2009. Early Paleozoic to Devonian multiple-accretionary model for the Qilian Shan, NW China. Journal of Asian Earth Sciences, 35: 323–333.

Zhang, M., He, Y., Chen, Z., and Gong, J., 2018. Analysis method and geological significance of C_5-C_7 light hydrocarbons in natural gas hydrate in permafrost, Qilian mountain. Petroleum Geology and Experiment, 40(3): 418–423 (in Chinese with English abstract).

Zhu, Y.H., Zhang, Y.Q., Wen H.J., Lu, Z.Q., and Wang, P.K., 2010. Gas hydrates in the Qilian Mountain permafrost and their basic characteristics. Acta Geoscientica Sinica, 31(1): 7–16 (in Chinese with English abstract).

Zumberge, J., Ferworn, K., and Brown, S., 2012. Isotopic reversal ('rollover') in shale gases produced from the Mississippian Barnett and Fayetteville formations. Marine and Petroleum Geology, 31(1): 43–52.

Zuo, Y.H., Wang, Q.F., Lu, Z.Q., and Chen, H., 2016. Tectono-thermal evolution and gas source potential for natural gas hydrates in the Qilian Mountain permafrost, China. Journal of natural gas science and engineering, 36(Pt.A): 32–41.

About the first and corresponding author

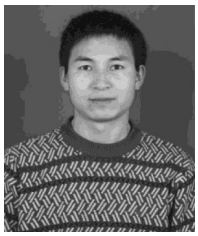

TAN Furong, male, born in 1984 in Hanzhong City, Shaanxi Province; master; graduated from Department of Geology, Northwestern university; Senior Engineer of Shaanxi Mineral Resources and Geological Survey. He is now interested in the study on organic geochemistry, paleoenvironment, and basin analysis of petroleum. Email: tanfurong1308@163.com; phone: 18691480996.

About the corresponding author

Li Yang, male, born in 1987 in Fengyang county, Anhui Province; Doctor; graduated from Northwest University; lecturer of Department of Geology, Northwest University. He is now interested in the studies on regional tectonics and natural resources. Email: liyangxbdx@163.com; phone: 18710572313.